Method to Generate Distribution Maps of the Material Parameters of the Human Body Using Robotic and Dynamic Simulation Systems

Takeharu Hoshi Yo Kobayashi Masakatsu G. Fujie

Waseda Unversity
59-309, 3-4-1, Ohkubo, Shinjuku, Tokyo, Japan
hoshi@aoni.waseda.jp

***Abstract*— The present paper proposes a new method by which to generate distribution maps of the material parameters of the human body for use in medical applications. In addition, a system design concept to realize the proposed method is presented, wherein the system integrates a robotic component and a numerical simulation component. The robotic component is used to measure the contact force and displacement at each point on the human body contacted by a robotic probe. The numerical simulation component generates an optimal distribution map of the material parameters using the proposed method, where three data are used, namely, (1) the measured data from the robotic part, (2) simulated deformation data obtained by the finite element method, and (3) distribution map data obtained using distribution models. In order to validate the proposed method, we implemented a virtual system including a sensing robot and a human body. We conducted numerical simulation experiments using this virtual system, and the results of experiments showed that optimal distribution maps were accurately generated.**

***Keywords*:** *Robotic surgery, Surgical simulation, Human tissue model, Material properties*

I. INTRODUCTION

A. Motivation

Computer assisted medical procedures are becoming ubiquitous in modern medicine [1], [2]. In particular, computer assisted dynamic simulation of the human body based on numerical human tissue models may have important applications in various medical situations. Examples of such applications include surgical planning systems, surgical training systems, and surgical robot control systems. Consequently, medical researchers have recently expressed great interest in technologies for the dynamic simulation of the human body.

Although computer assisted dynamic simulations have been expected to become widespread, practical methods by which to obtain appropriate and realistic simulation results have not yet been reported. This is primarily because determining the distribution of the material parameters of human tissues, which determine the accuracy of the dynamic simulation by the human tissue model, is generally difficult. This difficulty arises from two sources. First, there is no method by which to accurately, directly, and noninvasively measure the distribution of tissues for the entire human body. Second, individual differences in the properties of human tissues, which are related to factors such as age, sex, clinical history, and lifestyle, make it increasingly difficult to determine the values of the material parameters. Thus, if no method of determining the distribution of the material parameters of human tissues is developed, the use of computer assisted dynamic simulation may lead to a reliability problem from a medical point of view.

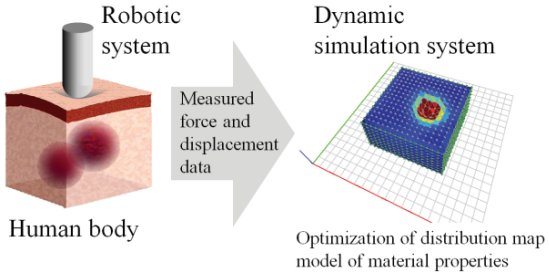

Fig. 1. Concept of the proposed method for generating a distribution map of the material parameters of the human body

In the present paper, we focus on the problem of the uncertainty of the distribution of the material parameters of human tissue models and propose a new method by which to generate optimal distribution maps of the material parameters of human tissues. In addition, we present a conceptual system design to realize the proposed method (Fig. 1). This system includes robotic and numerical simulation components. The robotic component is used to measure the contact force and displacement at each point on the human body contacted by a robotic probe. The dynamic simulation component identifies optimal distribution maps of material parameters based on the contact force and

displacement data measured by the robotic component. These components are described in detail in Section II.

B. Related Research

We briefly review research related to computer assisted dynamic simulation using human tissue models and material parameter identification problems.

1) Modeling and simulation of the human body: Various projects have investigated computer assisted dynamic simulation. Conventional studies on computer assisted dynamic simulation have focused on simulation for preoperative planning or teaching purposes [3], [4]. Recently, however, there has been a great deal of interest in simulation for intra-operative surgical robot control based on tissue models. For example, DiMaio *et al.* [5] proposed a system by which to measure the extent of planar tissue phantom deformation during needle insertion. Alterovitz *et al.* [6] investigated the simulation of needle insertion for prostate brachytherapy. Kobayashi *et al.* [7], [8] reported the material properties of the liver in order to realize physically accurate models and investigated physical organ modeling for use in a surgical robot control method.

2) Parameter identification problems: The uncertainty of the material properties of human tissue has been researched extensively. One solution to the problem of identifying the values of human material parameters is to use direct measurement devices that sample data directly from living human tissues. Ottensmeyer *et al.* [9] proposed a data acquisition tool for directly measuring the mechanical properties of tissues during surgery. Although this type of solution is helpful for confirming diagnoses, it is inherently invasive. An alternative, non-invasive approach is a measurement technique known as elastography that involves the use of static or oscillatory deformations [10]. Although it is certain that this technique will become a useful tool, it is likely that the primary concern of research in the field of elastography is to allow medical staff to visualize materials rather than to quantify the material parameters.

Studies dealing with the identification of material parameters of general objects have conventionally been reported in the areas of civil engineering or structural engineering research [11], [12]. In contrast to objects in these research areas, however, human tissues differ in various ways from earth ground or structural objects. As for research dealing with similar objects in the material properties of the human body, several research projects have investigated soft materials in recent years. Wang *et al.* [13] researched an identification method for rheological objects. The present authors addressed the problem of determining the values of human material parameters [14], [15]. The previously proposed algorithm [14], [15] was intended to modify the values of the material parameters iteratively, where we assumed that the spatial distribution of the tissues was known. In contrast to these studies, the objective of the present paper is to generate optimal distribution maps of the material parameters of human tissues.

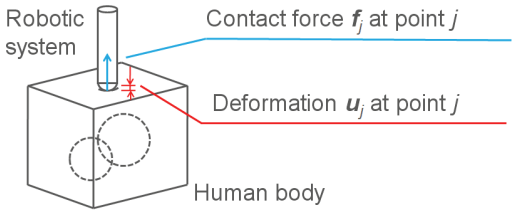

Fig. 2. Concept of the proposed robotic system for measuring the contact force and deformation

C. Contents

The remainder of the present paper is organized as follows. Section II introduces the proposed method and conceptual system design. Numerical experiments to verify the proposed method are described in Section III. Finally, Section IV presents the conclusion and describes areas for future research.

II. Method

In this section, we present a method by which to generate distribution maps of the material properties of the human body. The problem is defined, and a distribution map model is proposed. In addition, a deformation model is obtained by the finite element method (FEM), and a formulation to optimize the parameter of the distribution map model is proposed.

A. Problem Definition

The basic concept of the proposed method for generating distribution maps of the material parameters of human tissues is to compare the behavior of the simulation results obtained using tissue models with the actual deformations of tissues as obtained by a robotic sensing system. We take this strategy of the proposed method as a kind of problem of inverse analysis. The reason for this is that the distribution of the material parameters, which determines the behavior of human-body deformation, must be estimated from the available measurements, which are related to tissue deformation. The advantage of using a robotic sensing system is the ability to quantify measurement data. Generally speaking, robotic systems are useful as data acquisition tools. Therefore, we use a robotic system, which incorporates sensors for measuring the contact force and displacement at each point on the human body contacted by a robotic probe (Fig. 2).

Under the assumption of the existence of such a robotic system, we must formulate a method by which to generate the optimal distribution map of the material properties of the human body using measured data obtained by the robotic system. Next, we define the problem of determining the most appropriate distribution map of the material properties for the observed data.

One solution to this problem is to use optimization techniques. Here, we assume that the distribution map of the material properties, i.e., the values of the material parameter

m (e.g., Young's Modulus) at point $\boldsymbol{p}$, is formulated as follows:

$$m = m(\boldsymbol{p}, \boldsymbol{\theta}) \tag{1}$$

where $\boldsymbol{p} = (p_x, p_y, p_z)^{\mathrm{T}}$ is the position vector at any point of interest, and $\boldsymbol{\theta}$ is the parameter vector of the distribution map model, which we will define later in this section. Since the distribution map can be obtained with $\boldsymbol{\theta}$ by (1), $\boldsymbol{\theta}$ is the parameter vector to be optimized. The optimal parameter vector $\boldsymbol{\theta}^*$ is described as follows:

$$\boldsymbol{\theta}^* = \underset{\boldsymbol{\theta}}{\operatorname{argmin}} \left(J(\boldsymbol{\theta}) \right) \tag{2}$$

where $\boldsymbol{\theta}^*$ is obtained by minimizing the loss function $J(\boldsymbol{\theta})$, which is an indication of the degree of adaptation between the real deformation and the simulated deformation. An appropriate function by which to formulate the loss function is given by the sum of squares of errors as follows:

$$J(\boldsymbol{\theta}) = \frac{1}{2} \sum_j (y_j^{observation} - y_j^{model}(\boldsymbol{\theta}))^2 \tag{3}$$

where $y_j^{observation}$ and y_j^{model} are the values of the real and simulated deformation at the j^{th} point of measurement. Under these assumptions, the problem is how to formulate the simulated deformation y_j^{model} as a function of the parameter vector $\boldsymbol{\theta}$ of the distribution map. This problem is described in the following subsections.

B. Distribution Map Model

In this subsection, we modeled the distribution map of the material properties, i.e., the values of the material parameter m (e.g., Young's Modulus) in (1) at point $\boldsymbol{p}$. The human body has a distribution of material properties because the human body contains parenchyma tissues and underlying tissues, such as tumors. Thus, the effects of the underlying tissues must be modeled. Under these considerations, the material parameter m (e.g., Young's Modulus) in (1), which has a scalar value, can be modeled as follows:

$$m(\boldsymbol{p}, \boldsymbol{\theta}) = w_0^m + \sum_{i=1}^{n} (w_i^m * \emptyset_i(\boldsymbol{p})) \tag{4}$$

where the first and second terms on the right-hand side model the effects of the parenchyma and underlying tissues, respectively, n is the number of underlying tissues, $\boldsymbol{p} = (p_x, p_y, p_z)^{\mathrm{T}}$ is the position vector at any point of interest, w_0^m is a bias parameter of the material properties for parenchyma tissue, w_i^m is the weighting parameter of the effect of the i^{th} underlying tissue, and ϕ_i is a function to model the spatial effect of the i^{th} underlying tissue. Here, we modeled the effect of underlying tissues as a function of the distance from the center of underlying tissues, as follows:

$$\emptyset_i(\boldsymbol{p}) = \mathrm{h}(\|\boldsymbol{p} - \boldsymbol{q}_i\|) \tag{5}$$

where $\boldsymbol{q}_i = (q_{xi}, q_{yi}, q_{zi})^{\mathrm{T}}$ are the vector coordinates of the center position of the i^{th} underlying tissue. Given the consideration in (5), the class of the Gaussian function is one of the most suitable classes for the requirements. In the present paper, we modeled the function as follows:

$$\mathrm{h}(\|\boldsymbol{p} - \boldsymbol{q}_i\|) = \exp\left(-\frac{(\boldsymbol{p} - \boldsymbol{q}_i)^{\mathrm{T}}(\boldsymbol{p} - \boldsymbol{q}_i)}{2{r_i}^2}\right) \tag{6}$$

where r_i is an indicative distance of the effective area by the i^{th} underlying tissue. The conceptual scheme of (4) through (6) was illustrated in Figs. 3 and 4. Here, we derive the parameter vector $\boldsymbol{\theta}$ of the distribution model as follows:

$$\begin{aligned} \boldsymbol{\theta} = (& w_0^m, w_1^m, {\boldsymbol{q}_1}^{\mathrm{T}}, r_1, \\ & \ldots w_i^m, {\boldsymbol{q}_i}^{\mathrm{T}}, r_i, \\ & \ldots, w_n^m, {\boldsymbol{q}_n}^{\mathrm{T}}, r_i)^{\mathrm{T}} \quad , \quad i = 1, \ldots, n. \end{aligned} \tag{7}$$

In the next subsection, we relate the parameter $\boldsymbol{\theta}$ to the deformation model.

C. Deformation Model

Since the finite element method (FEM) is one of the most common methods by which to model dynamic behaviors, in the present study, we use the FEM to model the deformation of human tissues. In the FEM theory, the element stiffness matrix K^e, which expresses the local stiffness, is given as

$$\boldsymbol{K^e} = \int_{V^e} \boldsymbol{B}^{e\mathrm{T}} \boldsymbol{C}^e \boldsymbol{B}^e \, \mathrm{d}V^e \tag{8}$$

where $\boldsymbol{B}^e$ is the matrix that relates the strain and displacement, V^e is the volume of the element, and $\boldsymbol{C}^e$, which is referred to as the material matrix, is the matrix defined by the material parameters. In particular, if the element of the FEM is a four-node tetrahedral, elastic, and isotropic element, the material matrix $\boldsymbol{C}^e$ is written as:

$$\boldsymbol{C}^e = \begin{bmatrix} \lambda^e + 2\mu^e & \lambda^e & \lambda^e & 0 & 0 & 0 \\ \lambda^e & \lambda^e + 2\mu^e & \lambda^e & 0 & 0 & 0 \\ \lambda^e & \lambda^e & \lambda^e + 2\mu^e & 0 & 0 & 0 \\ 0 & 0 & 0 & \mu^e & 0 & 0 \\ 0 & 0 & 0 & 0 & \mu^e & 0 \\ 0 & 0 & 0 & 0 & 0 & \mu^e \end{bmatrix} \tag{9}$$

where λ^{e} and μ^{e} are the Lame material constants at the local position, given by the Young's modulus E^e and the Poisson's ratio ν^e:

$$\lambda^e = \frac{\nu^e E^e}{(1 + \nu^e)(1 - 2\nu^e)} \quad , \quad \mu^e = \frac{E^e}{2(1 + \nu^e)} \, . \tag{10}$$

In this case, the deformation is solved using the following equation:

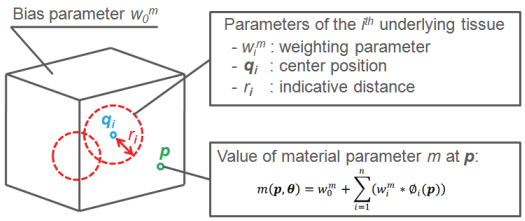

Fig. 3. Modeling the effects of underlying tissues

$$\underline{\boldsymbol{u}} = \boldsymbol{K}^{-1}\underline{\boldsymbol{f}} \tag{11}$$

where $\boldsymbol{K}$, which is referred to as the global stiffness matrix, is calculated as the total of the element stiffness matrix $\boldsymbol{K}^e$. Thus, $\boldsymbol{K}$ is also associated with the material parameters E^e and ν^e at each nodal point. In (11), $\underline{\boldsymbol{u}}$ and $\underline{\boldsymbol{f}}$ are the discretized displacement vector and the force vector, respectively, at each nodal point in the FEM model.

Next, based on the fact that K is associated with the material parameters, the displacement vector $\underline{\boldsymbol{u}}$ can be related to the parameters of the distribution model:

$$\underline{\boldsymbol{u}} = \underline{\boldsymbol{u}}(\boldsymbol{K}(\boldsymbol{\theta}), \underline{\boldsymbol{f}}). \tag{12}$$

Here, since $\underline{\boldsymbol{u}}$ is a function of $\boldsymbol{\theta}$, it can be used for the calculated information $y_i^{model}(\boldsymbol{\theta})$ in (3).

D. Optimization of the Distribution Map Model

Here, we consider the method by which to optimize the parameter in (2). In the present paper, we use the Broyden Fletcher Goldfarb Shanno (BFGS) quasi-Newton method to minimize the loss function and concurrently optimize the parameters of the distribution map model. Typically, this quasi-Newton method is a fast, general-purpose optimization approach for solving nonlinear problems. This method seeks a point at which the gradient of an evaluation function is the zero vector. The framework to optimize the parameters of distribution map model is shown in Fig. 5.

III. Numerical Experiment

A. Overview

In this section, we describe the results of numerical experiments that were conducted in order to assess the feasibility of the generality of the proposed system. We implemented a virtual system that incorporates a sensing robot and a human body. The virtual sensing robot provides pseudo-measurement data. In this experiment, we used this pseudo-data instead of physical data. This type of numerical experiment using pseudo-data, which is generally referred to as an identical twin experiment, is performed in order to verify the model and to examine the sensitivity of the model results.

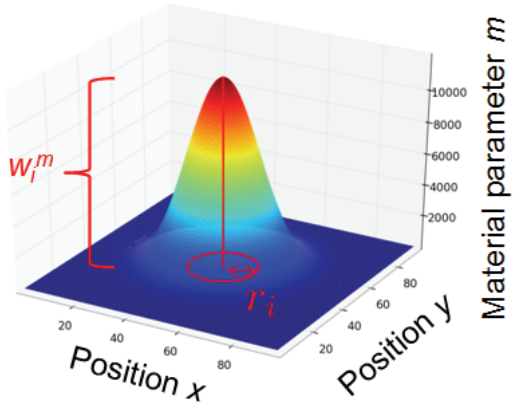

(a)

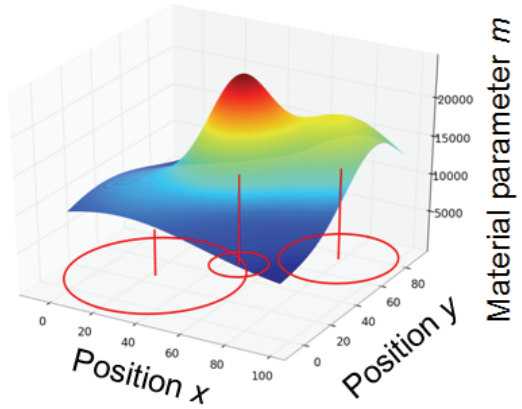

(b)

Fig. 4. Modeling of the distribution map of the material parameter. The indicative distance parameter r is shown by the red circles. (a) Example of the effect of an underlying tissue. (b) Example of the effect of three underlying tissues

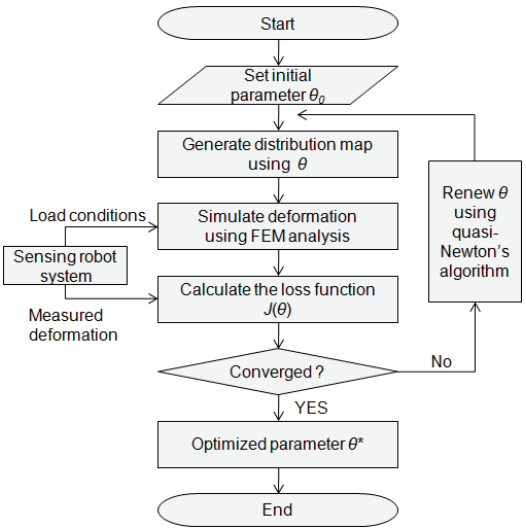

Fig. 5. Framework for optimizing the parameters of the distribution map model

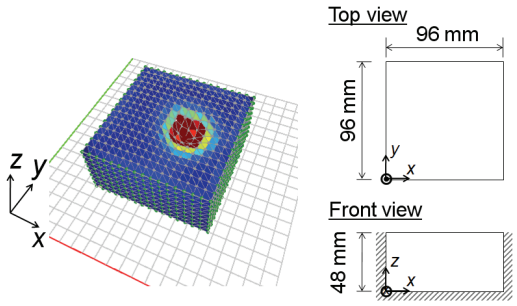

Fig. 6. Proposed FEM deformation simulator

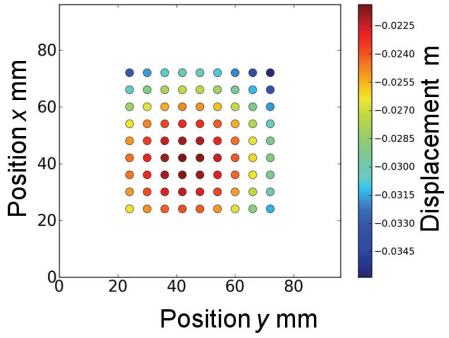

Fig. 7. Example of calculated displacement at the contact points obtained by the FEM software

B. Experimental conditions

The experiments were conducted under the following conditions.

1) Deformation Model using FEM: The proposed FEM simulator for calculating the deformation was implemented in C++ and, in part, Python (Fig. 6). The simulator is used to examine three-dimensional solids constructed of four-node linear tetrahedron elements. The FEM model in the present experiment includes 2,601 nodes and 12,288 elements. In the experiment, the FEM model is a hexahedron of 96 mm in width, 96 mm in depth, and 48 mm in height.

2) Distribution Map Model: In these experiments, we choose the Young's modulus as the material property to be analyzed because the Young's modulus is one of the most important material parameters of the human body in the deformation problem. Based on Eqs. (4) through (7), the distribution of the Young's Modulus at point $\boldsymbol{p}$ is calculated as follows:

$$E(\boldsymbol{p},\boldsymbol{\theta}) = w_0^E + \sum_{i=1}^{n}\left(w_i^E * \exp\left(-\frac{(\boldsymbol{p}-\boldsymbol{q}_i)^{\mathrm{T}}(\boldsymbol{p}-\boldsymbol{q}_i)}{2{r_i}^2}\right)\right) \tag{13}$$

where $\boldsymbol{\theta} = (w_0^E,\ w_1^E,\ \boldsymbol{q}_1^{\mathrm{T}}, r_1,\ \ldots,\ w_i^E,\ \boldsymbol{q}_i^{\mathrm{T}}, r_i,\ \ldots,\ w_n^E,\ \boldsymbol{q}_n^{\mathrm{T}}, r_n)^{\mathrm{T}}$ is the parameter vector to be optimized.

TABLE I

EXPERIMENTAL CONDITIONS

Test	status	w_0^E Pa	w_1^E Pa	$(q_{x1},\ q_{y1})$ mm	r_1 mm
I	initial	**(1)7200 (2)4800**	**(1)14400 (2)9600**	48, 48 (const.)	12 (const.)
	correct	6000	12000		
II	initial	6000	12000	**46, 46**	12
	correct	(const.)	(const.)	**60,60**	(const.)
III	initial	6000	12000	48, 48	**12**
	correct	(const.)	(const.)	(const.)	**24**
IV	initial	6000	12000	**48, 48**	**6**
	correct	(const.)	(const.)	**60, 60**	**24**
V	initial	**7200**	**14400**	**(48, 48)**	**12**
	correct	**6000**	**12000**	**48, 48**	**24**

In this experiment, in the initial approximation, we assume the Poisson's ratio to be constant at $\nu^e = 0.49$ at each element due to the incompressible property of the human body.

3) Pseudo-observation Data Sets: In a numerical experiment, we used pseudo-observation data sets of force and displacement. The parameters $\boldsymbol{\theta}^{\text{correct}}$, which, as a matter of convenience, are referred to herein as the correct parameters, generate the pseudo-distribution data, which are set to FEM simulator. These parameters are expressed as follows:

$$\begin{aligned}\boldsymbol{y}^{\text{pseudo-observaion}} &= \underline{\boldsymbol{u}}(\boldsymbol{K}(\boldsymbol{\theta}^{\text{correct}}), \underline{\boldsymbol{f}})\\ \boldsymbol{\theta}^{\text{correct}} &= (w_0^{E\text{correct}},\ w_1^{E\text{correct}},\ \boldsymbol{q}_1^{\text{correct T}}, r_1^{\text{correct}},\\ &\quad \ldots,\ w_i^{E\text{correct}},\ \boldsymbol{q}_i^{\text{correct T}}, r_i^{\text{correct}},\\ &\quad \ldots,\ w_n^{E\text{correct}},\ \boldsymbol{q}_n^{\text{correct T}}, r_n^{\text{correct}})^{\mathrm{T}}.\end{aligned} \tag{14}$$

In the experiments, the values of the contact forces between the virtual robot and the virtual human body were set to be 3 N. A total of 81 points on the top surface of the virtual human body were designated as contact points to measure the displacements (Fig. 7).

3) Experimental Conditions: We conducted six tests with different conditions. The values of these parameters are generally on the same order as those of human tissues. Each of the six tests was designed to evaluate the proposed method from a unique perspective. The initial and correct values of the parameters to generate the distribution maps for the five tests are listed in Table I. In five of the tests, we assumed the number of underlying tissues to be one, and in one of the tests, we assumed the number of underlying tissues to be two. In all six tests, q_{zi}, which is the z-direction center position of the i^{th} underlying tissue, is set to be constant (36 mm) in order to focus attention on the other direction positions, namely, q_{xi} and q_{yi}.

Note that, in the optimization algorithm, the values of the parameters are modified to strengthen the stability of the numerical analysis by maintaining the scales of the parameters to be the same.

The experimental conditions are described in detail below.

1) Test I: In this test, we evaluate the ability to concurrently optimize the Young's modulus in the surrounding parenchyma tissue and the underlying tissue. Here, the parameter to be optimized is $\boldsymbol{\theta} = (w_0^E, w_1^E)^{\mathrm{T}}$.

2) Test II: In this test, we evaluate the ability to optimize the center position $\boldsymbol{q}_1$ of the underlying tissue. Here, the parameter to be optimized is $\boldsymbol{\theta} = (q_{x1}, q_{y1})^{\mathrm{T}}$.

3) Test III: In this test, we evaluate the ability to optimize the indicative distance r_1 for the effective area of the underlying tissue. Here, the parameter to be optimized is $\boldsymbol{\theta} = (r_1)$.

4) Test IV: In this test, we evaluate the ability to concurrently optimize the center position $\boldsymbol{q}_1$ and the indicative distance r_1 for the effective area of the underlying tissue. Here, the parameter to be optimized is $\boldsymbol{\theta} = (q_{x1}, q_{y1}, r_1)^{\mathrm{T}}$.

5) Test V: In this test, we evaluate the ability to concurrently optimize all of the parameters considered in Tests I through IV. Here, the parameter to be optimized is $\boldsymbol{\theta} = (w_0^E, w_1^E, q_{x1}, q_{y1}, r_1)^{\mathrm{T}}$.

6) Test VI: In this test, we assume the existence of two underlying tissues. We evaluate the ability to concurrently optimize the center positions $\boldsymbol{q}_1$ and $\boldsymbol{q}_2$ of the underlying tissues. Here, the parameter to be optimized is $\boldsymbol{\theta} = (q_{x1}, q_{y1}, q_{x2}, q_{y2})^{\mathrm{T}}$. The correct parameter values are as follows: $w_0^{Ecorrect} = 6{,}000$ Pa, $w_1^{Ecorreet} = w_2^{Ecorreet} = 12{,}000$ Pa, *and* $r_1^{correct} = r_2^{correct} = 12$ mm.

C. Results and Discussion

The results of the numerical experiment are shown in Figs. 8 through 13. The parameters were found to converge to the correct values quite well. Therefore, the effectiveness of the proposed method was shown through the results of the numerical experiments.

IV. Conclusion

The present study proposed new concepts for generating distribution maps of the material parameters of the human body. The proposed system incorporates a robotic sensing system and a numerical dynamic simulation system. The method and formulation of the proposed system were also described herein. The distribution map was modeled by summing Gaussian functions that express the effects of underlying tissues. An FEM model was used as a numerical dynamic simulator. Numerical experiments carried out in order to demonstrate the feasibility of the proposed method. The experimental results revealed that the proposed method of

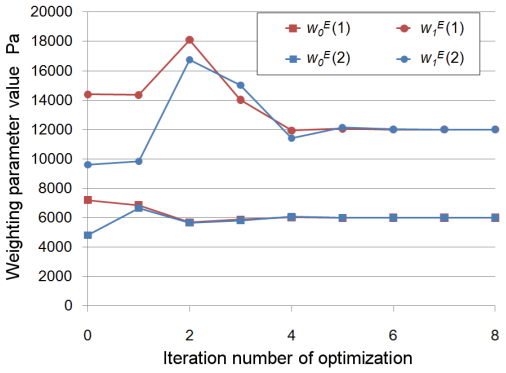

Fig. 8. Results of Test I. The weighting parameters, w_0^E and w_1^E, converged to the correct values in both tissues.

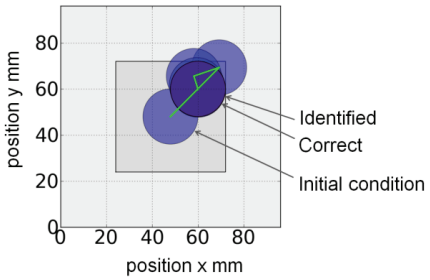

Fig. 9. Results of Test II. The center position, $\boldsymbol{q}_1$, converged to the correct value.

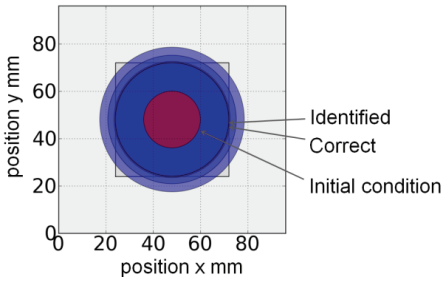

Fig. 10. Results of Test III. The indicative distance, r_1, converged to the correct value.

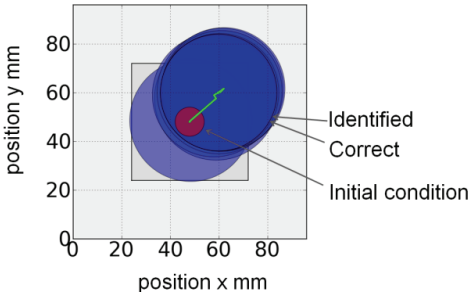

Fig. 11. Results of Test IV. The center position, $\boldsymbol{q}_1$, and the indicative distance, r_1, converged to the correct values.

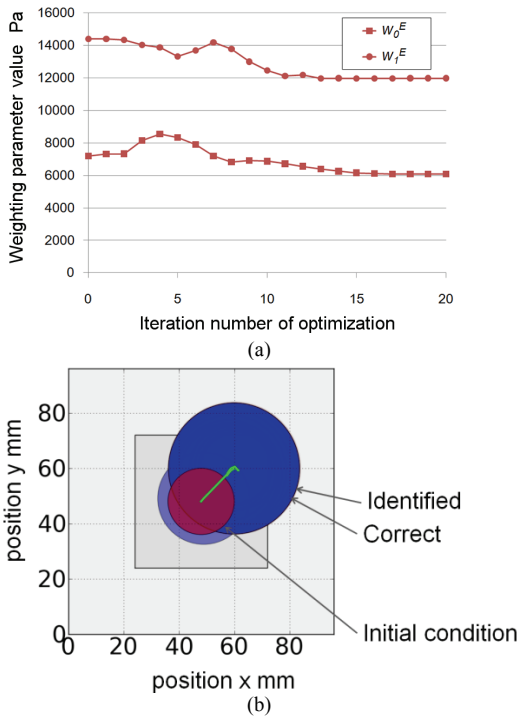

Fig. 12. Results of Test V. The weighting parameters, w_0^E and w_1^E (shown in (a)), the center position, $\boldsymbol{q}_1$, and the indicative distance, r_1 (shown in (b)), converged to the correct values.

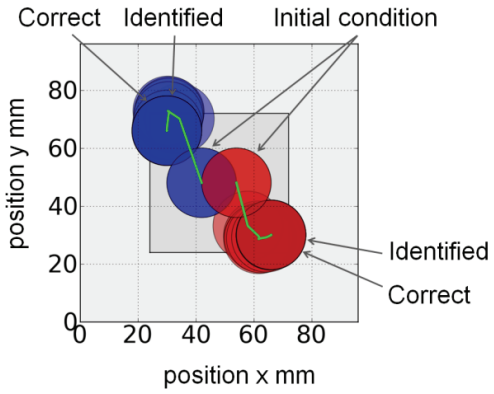

Fig. 13. Results of Test VI. The center positions, $\boldsymbol{q}_1$ and $\boldsymbol{q}_2$, of the two underlying tissues converged to the correct values.

generating the distribution map provided a correct distribution map, thereby validating the proposed method.

In the future, we intend to develop an actual system that integrates a robotic system and a dynamic simulation system for medical applications. System integration of a robotic system and a computer aided engineering system is one of the key concepts of the present study. The proposed method is an important step toward realizing a fully integrated system.

ACKNOWLEDGEMENT

The present study was supported in part by the Ministry of Education, Culture, Sports, Science and Technology of Japan (MEXT) through the Global COE Program “Global Robot Academia” and as a High-Tech Research Center Project.

REFERENCES

[1] P. Dario, E. Guglielmelli, B. Allotta, M.C. Carrozza, "Robotics for medical applications," Robotics & Automation Magazine, IEEE, vol.3, no.3, pp.44-56, Sep 1996

[2] R. H. Taylor, D. Stoianovici, "Medical robotics in computer-integrated surgery," Robotics and Automation, IEEE Transactions on , vol.19, no.5, pp. 765-781, Oct. 2003

[3] Stephane Cotin, Herve Delingette, and Nicholas Ayache, "Real-Time Elastic Deformations of Soft Tissues for Surgery Simulation," IEEE Transactions on Visualization and Computer Graphics, Vol. 5, No. 1, 1999

[4] Morten Bro-Nielsen, "Finite element modeling in surgery simulation," Proceedings of The IEEE, Vol. 86, pp. 490-503, 1998

[5] Simon P. DiMaio and Septimiu E. Salcudean, "Interactive Simulation of Needle Insertion Models," In IEEE Transaction on Biomedical Engineering,Vol. 52, No. 7, 2005, pp. 1167-1179

[6] Ron Alterovitz, Ken Goldberg, and Allison Okamura, "Planning for Steerable Bevel-tip Needle Insertion Through 2D Soft Tissue with Obstacles," in Proc. IEEE International Conference on Robotics and Automation (ICRA), Apr. 2005, pp. 1652-1657

[7] Yo Kobayashi, Akinori Onishi, Takeharu Hoshi, Kazuya Kawamura, and Masakatsu G. Fujie, "Viscoelastic and Nonlinear Organ Model for Control of Needle Insertion Manipulator, " In International Conference of the IEEE Engineering in Medicine and Biology Society, pp. 1242-1248, 2007

[8] Y. Kobayashi, T. Hoshi, K. Kawamura and M. G. Fujie, "Control Method for Surgical Robot to Prevent Overload at Vulnerable Tissue," In IEEE International Conference on Robotics and Automation, pp. 1893-1899, 2007

[9] Mark P. Ottensmeyer and J. Kenneth Salisbury Jr., "In Vivo Data Acquisition Instrument for Solid Organ Mechanical Property Measurement," Medical Image Computing and Computer Assisted Intervention MICCAI 2001, pp. 975-982

[10] J. Ophir, S. K. Alam, B. Garra, F. Kallel, E. Konofagou, T. Krouskop, T. Varghese, "Elastography: ultrasound estimation and imaging of the elastic properties of tissues," Proceedings of the Institution of Mechanical Engineers, Part H: Journal of Engineering in Medicine, Volume 213, Number 3 / 1999, pp. 203-233

[11] S. Aoki, K. Amaya, M. Sahashi, T. Nakamura, "Identification of Gurson's material constants by using Kalman filter," Computational Mechanics, vol 19, pp. 501-506 1997

[12] Yu Gu, Toshio Nakamura, Lubos Prchlik, Sanjay Sampath, Jay Wallace, "Micro-indentation and inverse analysis to characterize elasticplastic graded materials," Materials Science and Engineering, vol 345, 2003, pp. 223-233

[13] Zhongkui Wang, Kazuki Namima, and Shinichi Hirai, "Physical Parameter Identification of Rheological Object Based on Measurement of Deformation and Force," in 2009 IEEE International Conference on Robotics and Automation, pp. 1238 -1243

[14] T. Hoshi, Y. Kobayashi, K. Kawamura, M. G. Fujie, "Developing an Intraoperative Methodology Using the Finite Element Method and the Extended Kalman Filter to Identify the Material Parameters of an Organ Model," 29th Annual International Conference of the IEEE Engineering in Medicine and Biology Society, pp.469-474, 2007

[15] T. Hoshi, Y. Kobayashi, M. G. Fujie, "Developing a system to identify the material parameters of an organ model for surgical robot control," 2nd IEEE RAS & EMBS International Conference on Biomedical Robotics and Biomechatronics (BioRob), pp.730-735, 2008